Population-Based SHM Under Environmental Variability Using a Classifier for Unsupervised Damage Detection

YACINE BEL-HADJ and WOUT WEIJTJENS

ABSTRACT

In this paper, we introduce a novel deep learning technique for anomaly detection in the context of Population-Based Structural Health Monitoring (PB-SHM). The proposed method eliminates manual feature engineering by utilizing Power Spectral Density (PSD) as input, allowing examination of the entire spectrum. It is based on an auxiliary classification task, wherein the model is trained to discriminate between different systems according to their dynamic response. The classifier confidence is then used during inference for damage detection. The neural network extracts discriminative features commonly impacted by damage, which are employed to create a normality model. The efficacy of our method is demonstrated on a simulated population of 20 individual 8-DOF systems influenced by a latent environmental variables, emphasizing its potential for PB-SHM under diverse conditions. Our technique achieves performance comparable to resonance frequency-based methods while potentially exhibiting higher capability in complex structures with multiple modes. Anomalies caused by a 5% decrease in stiffness are successfully detected, yielding an AUC of 0.94.

INTRODUCTION

Structural Health Monitoring (SHM) plays a crucial role in ensuring the safety, reliability, and performance of complex engineering structures across various applications. SHM techniques aim to detect and analyze damage in structures, enabling the implementation of strategies to increase component service life and prevent catastrophic failure [1]. Vibration-based monitoring has emerged as a primary focus in SHM for damage detection, as damage alters structural characteristics, such as stiffness, which are reflected in the measured vibration response of the structure [2]. Consequently, signal processing techniques capable of extracting damage-sensitive features from vibration signals and identifying subtle changes over time have been recurring examples of SHM solutions. Additionally, accounting for Environmental and Operational Conditions (EOC) is necessary since EOCs can induce changes in damage-sensitive features similar in magnitude to those caused by damage [3].

Yacine Bel-Hadj, PhD Student, Email: yacine.bel-hadj@vub.be. Vrije Universiteit Brussel (VUB), OWI-lab, Department of Applied Mechanics (MECH), Pleinlaan 2, 1050 Brussels

Historically, SHM research has relied on feature engineering, which revolve around computing predefined features and performing statistical analysis thereon to account for EOCs [4]. As features are engineered to target specific anomalies, they are not failure mode agnostic, necessitating custom features for different SHM applications. Various features have been used for damage detection, such as cross-correlation of measured data [5], modal parameters [6], including those obtained from operational modal analysis (OMA) [7]. Auto-encoders have also been employed for novelty detection in SHM data, utilizing environmental data and modal parameters to train normality models [8].

These traditional SHM solutions, which depend on feature engineering, are powerful but time-consuming and require significant knowledge of the structure. Recent research has shifted focus to SHM models that eliminate the need for extensive feature engineering and ad hoc hypotheses for failure modes [9, 10].

An additional opportunity to potentially improve anomaly detection systems might arise from the increasing amount of SHM data that is being collected on similar structures, e.g. wind turbines. Population-based SHM (PB-SHM) is an emerging field that focuses on transferring knowledge from one structure to another with minimal data [11]. Inspired from the work of [11], this contribution develops a novel deep learning approach for anomaly detection in the context of population-based SHM, utilizing an auxiliary classification task. Our method uses Power Spectral Density (PSD) as input, providing a comprehensive view of the structure's state without measuring environmental variables or manual feature engineering. We validate our approach on a simulated population of 20 individual 8-DOF systems affected by simulated environmental variables, demonstrating its potential for PB-SHM, particularly in the presence of environmental variability.

The work proposed in this paper is inspired from the recent research on out-of-distribution detection where the goal is to ensure the reliability and safety of deep learning [12].

DATASET

In this study, we utilize a dataset generated from twenty 8-degree-of-freedom (DOF) systems to evaluate our proposed structural health monitoring (SHM) strategy. This section will detail the system description and simulation process, forming the basis for model implementation and evaluation.

System Description

In this research, the data used was inspired by a study conducted in [11]. The 8-degree of freedom (DOF) population was created by first designing an ideal system, which served as the basis for generating 20 members with minimal variations in parameter values to simulate construction variability. As highlighted in [11], the resulting population was classified as strongly homogeneous.

A schematic illustration of the 8-DOF system is shown in Figure 1, where $u_j(t)$ and $z_j(t)$ represent the input and output acceleration of mass j at time t, respectively. In addition to the variation between the individuals introduced in [11], we also added a variation due to a latent variable that affected the stiffness of each element of the structure to model the effect of environmental conditions on the structure, e.g. Temperature.

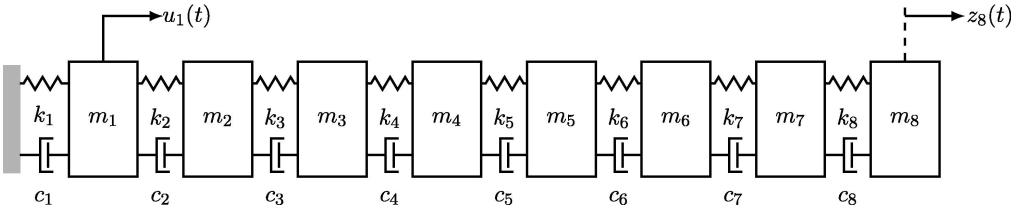

Figure 1. A schematic representation of the 8-dof [11]

TABLE I. SYSTEM PARAMETERS

j	1	2	3	4	5	6	7	8
$m_j(kg)$	0.5318	0.4040	0.4101	0.4123	0.3960	0.3809	0.4086	0.3798
$k_j(kN/m)$	1e-6	56.70	56.70	56.70	56.70	56.70	56.70	56.70
$c_j(Ns/m)$	8.7460	8.7916	8.8012	8.8512	8.7146	8.7378	8.5494	8.7521
$\alpha_j(kN/m)$	1e-9	-20	-20	350	-30	-350	100	-45

We modeled the effect of the latent variable on stiffness through a linear relationship, where $k_j^{'(i)}(l)$ is the new value of $k_j^{(i)}$ of the j^{th} spring of the i^{th} individual of the population after considering the latent environmental effect, the used equation to model the effect of environment is as follows $k_j^{'(i)}(l) = k_j^{(i)} - \alpha_j^{(i)} \cdot l$. Here, l is the latent environmental variable, and $\alpha_j^{(i)}$ is the coefficient that models the latent variable effect of the j^{th} spring of the i^{th} individual. Each member of the population is associated with individual attributes represented by $\Theta_i = \left\{m_j^{(i)}, k_j^{(i)}, c_j^{(i)}, \alpha_j^{(i)}\right\}_{j=1}^{8}$, where the index i refers to each individual of the population. To generate a strongly homogeneous group, the densities $P(\Theta i)$ that describe the underlying distribution of these parameters were modeled as Gaussian distributions with low dispersion. The system parameters for the ideal 8-DOF system were listed in Table I. A strongly homogeneous population was generated by sampling 20 parameter sets Θ_i from the distributions as shown in equation 1, defining the 20 similar members.

$$\begin{aligned} m_j^{(i)} &\sim \mathcal{N}\left(m_j, 0.03 \times m_j\right), \quad & k_j^{(i)} &\sim \mathcal{N}\left(k_j, 0.01 \times k_j\right) \\ c_j^{(i)} &\sim \mathcal{N}\left(c_j, 0.08 \times c_j\right), \quad & \alpha_j^{(i)} &\sim \mathcal{N}\left(\alpha_j, 0.01 \times \alpha_j\right) \end{aligned} \tag{1}$$

Figure 2 illustrates the impact of the latent variable on the system dynamics. It can be seen that as the value of the latent variable increases, the transfer function between mass 8 and mass 1 is affected. The selection of α_j was based on the intention to produce varying effects of the environmental variable on different modes of the system. Some modes affected by increased values while others by decreased resonance frequency. Additionally, the relationship between the modes and the latent variable was designed to be non-uniform, with some modes exhibiting a linear relationship with the latent variable while others exhibit a quadratic relationship. To simulate anomalies in the system, we reduced the stiffness k_5 by 1%, 3% ...13%. The effect of anomalies on the transfer function $|H(1,8)|$ is shown in Figure 3, we observe that this anomaly mainly affects the last mode(s). Consistent with real-world experience, the variation induced by the latent variable far exceeds the effect of the considered anomalies in the system. As a result it will be difficult to detect damage without EOC compensation.

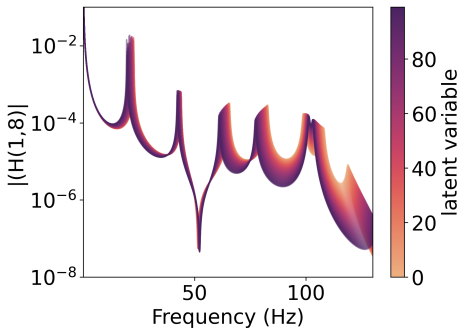

Figure 2. System variability of a single member of the population due the latent environmental variable

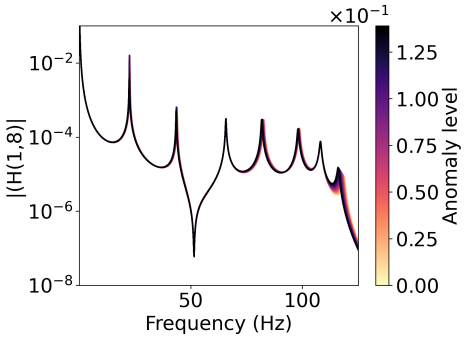

Figure 3. The effect of the anomaly on the system transfer function $|H(1,8)|$ of a single member of the population

Simulation

In this study, we utilize a dataset comprising a population of twenty 8-degree-of-freedom (DOF) systems. Each system is subjected to excitation with white noise at the first degree of freedom ($u_1(t)$), while the acceleration of the eighth mass ($z_8(t)$) is computed. To introduce variability in the system's excitation, we sample the excitation amplitude for each simulation from a Weibull distribution. The Weibull distribution is defined by the following parameters: shape parameter ($k = 1.9$), scale parameter ($\lambda = 5$), and location parameter ($\theta = 10$). Consequently, the excitation amplitude distribution exhibits a mean of 14.5 N and spans a range of 10 N to 30 N. Additionally, to simulate varying environmental conditions across simulations, we introduce variability in the latent environmental variable. The latent environmental variable is sampled from a normal distribution with a mean ($\mu = 50$) and a standard deviation ($\sigma = 30$).

The simulations are conducted for a total duration of 10 seconds, with a sampling frequency of 400 Hz. The Power Spectral Density (PSD) of the eighth mass is computed using the Welch algorithm [13] implemented in the Scipy package [14]. The dataset comprises 1,200 normal-condition samples per system, along with an additional 200 samples for each anomaly level, resulting in a total of 2,600 simulations per system. Out of the normal-condition samples, 600 samples are allocated for testing, while the remaining 600 samples are used for model fitting. In total, the dataset consists of 52,000 samples for the entire population.

MODEL IMPLEMENTATION

This section presents the proposed SHM strategy and a baseline approach for comparison. The objective is to address the anomaly detection problem with minimal preprocessing and feature engineering. In a final SHM schema, these two approaches are complimenting each other not competing.

Proposed Approach

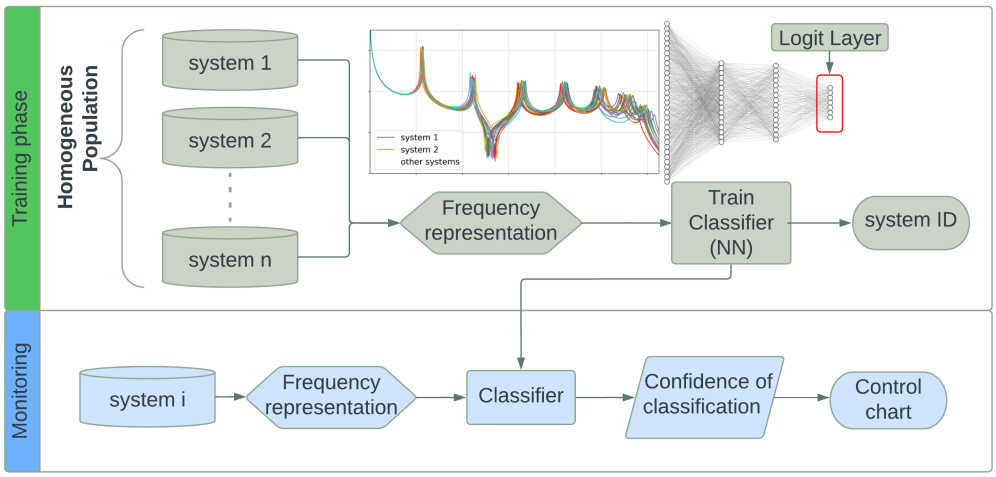

Figure 4. Flowchart illustrating the implementation of DeepSpectra Anomaly Detection (DSAD)

This section presents the proposed approach, referred to as the DeepSpectra Anomaly Detection (DSAD) method, for anomaly detection in the context of population-based SHM. The proposed approach utilizes the frequency representation of acceleration data as input and trains a neural network model to distinguish between each system based on the content of their PSD.

To obtain the PSD, To obtain the PSD, a window of 1024 samples is used with the p-Welch algorithm, taking into account the sampling frequency of 400Hz, the resulting frequency resolution is 0.39Hz. Prior to inputting them into the model, the PSDs are subjected to log and min-max normalization. The neural network architecture employed in this study consists of six dense layers with the following dimensions: [512, 256, 128, 64, 32, 20]. To enhance model stability during training, L_1 regularization is applied to the weights of the layers, and Batch Normalization regularization is incorporated between layers. The decision to incorporate these regularization techniques is based on previous studies on understanding the role of regularization methods in machine learning [15, 16].

In the training phase, the model is trained to classify the PSD into the different systems from where they are generated. This auxiliary task allows the model to learn a discriminative set of features of the input signal. The assumption is that the features that allow to discriminate between systems are those that typically become affected by damage (i.e. zeroes and poles). Figure 4 illustrates the methodology, which shows a clear separation between the training and monitoring (or inference) stages of the approach.

The final layer (logit layer in Figure 4) of the model contains 20 neurons, corresponding to the 20 different systems, and a Softmax function is applied as an activation function, scaling logits into probabilities[17]. The neuron with the highest activation in the final layer dictates the system predicted by the model. To visualize the learned embedding of the penultimate layer (before the logit layer), we project it into a lower-dimensional space using Uniform Manifold Approximation and Projection (UMAP) [18]. UMAP, a nonlinear dimensionality reduction method, visualizes clusters or groups of data points and their relative proximity. Figure 5 displays the UMAP visualization of the penultimate layer's embedding, with the original 32-dimensional embedding of the penultimate

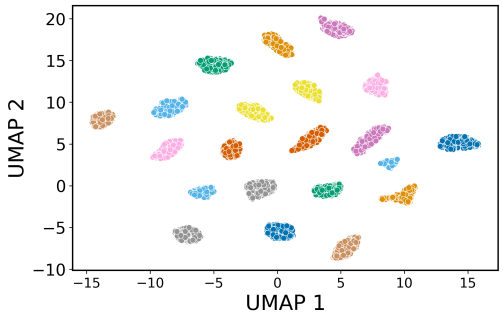

Figure 5. UMAP visualization of the penultimate layer's embedding. Each color represents a distinct system in the population.

layer mapped to two dimensions. The figure demonstrates how the model has learned a feature set, inferring each system to a distinct cluster.

Lastly, the anomaly index is defined based on the penultimate layer's embedding of the inferred PSD. Although one could use the Softmax-normalized value as a proxy for the model's aleatoric uncertainty (uncertainty arising from data, as opposed to epistemic uncertainty resulting from the model), relying on Softmax to quantify model certainty can be problematic, as detailed in [15]. Therefore, we employ a Gaussian Mixture Model (GMM) in the penultimate layer. We fit the GMM using the training data's embedding, setting the number of mixture components equal to the population size, which in this case is 20. The log-likelihood of the inferred PSD in the embedding under the mixture is then used as an anomaly index.

Baseline Approach

To compare the performance of the novel method, we also implement a solution using the system's resonance frequencies as damage sensitive engineered features. We compute the exact resonance frequency of the different systems, excluding the first mode of the system at 8e-5 Hz. We then add Gaussian noise with a standard deviation of 0.2Hz, as real-life situations only provide an estimation of the value. This results in a relative error of less than 1% for 68% of the time for the second mode at 20Hz. The anomaly is detected by recognizing a shift in the resonance frequency.

As our simulation includes environmental effects, it is essential to eliminate these effects to prevent masking the resonance frequency variations caused by anomalies. We employ a PCA-based approach to identify a linear subspace where environmental effects are located and compute the residual of the projection onto this subspace to remove the environmental effects[3]. The Scree plot criterion [19], also known as the 'elbow rule', is utilized to determine the number of principal components to consider. The intention is not to compete with the baseline method, as one is feature-based and the other considers the entire spectrum. These two methods perform better when complementing each other. The objective here is to have a better quantification of the performance of the proposed approach w.r.t. a commonly accepted strategy for SHM.

DISCUSSION OF THE RESULT AND COMPARISON

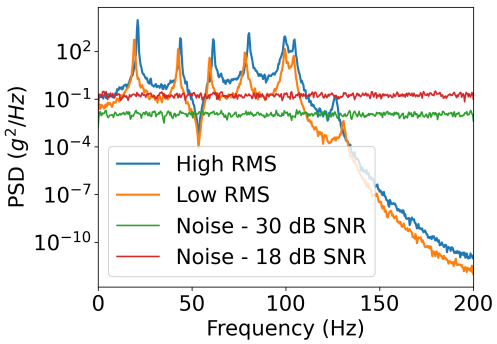

Figure 6. PSD Examples: Comparing High and Low RMS Signals with Noise at SNR of 18 and 30 dB

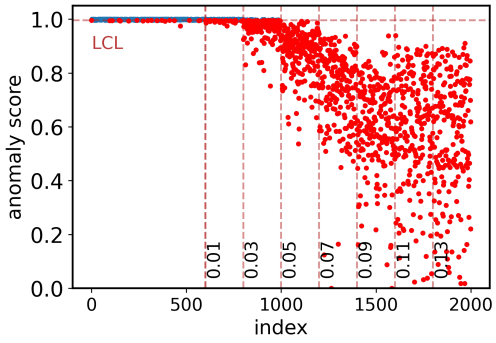

Figure 7. Control Chart for System 1, Using Only Test Data.Vertical lines represent different anomaly levels.

In this section, we evaluate the models' performance using the well-known Area Under the Curve (AUC) metric, which considers the distribution of healthy and anomalous datasets. A higher AUC indicates better separation between these distributions, with a perfect detector achieving an AUC of 1 and random assignment resulting in an AUC of 0.5. The AUC can also be interpreted as the probability of detecting an anomaly when the inferred point is anomalous. We argue that the AUC metric can be somewhat strict in the context of SHM. While a higher AUC indicates quicker anomaly detection, it is important to note that even with a moderately low AUC e.g. 0.7, the anomaly may not be immediately apparent. However, in the context of SHM one can assume anomalies to be persistent and remain present over time, the shift in the anomaly index can gradually become more evident, eventually leading to anomaly detection.

Performance Evaluation and Comparison of Anomaly Detection Approaches

We consider two scenarios in this study. The first scenario involves the dataset without any additional noise to the PSD. Where variations in the dataset primarily attributed to latent environmental factors, excitation fluctuations, and population differences. In the second scenario, we add a constant power noise to the signals through the whole dataset, resulting in SNRs of 10, 18, and 30 dB for a signal with an RMS equal to the 5^{th} percentile of the entire dataset. Figure 6 displays the PSD plots of two signals with extreme RMS values. The signal with a low RMS corresponds to the 5th percentile of the RMS distribution, while the blue PSD corresponds to the 95th percentile. It is evident that the noise with an SNR of 18 dB floods the higher-order mode, which is the most sensitive to damage. To account for this in the baseline approach, the eighth-order mode is disregarded. We compute the AUC between the training data and healthy testing data, and subsequently, the AUC using the 200 samples of the healthy testing data and anomalous data for each anomaly level. Table II provides a performance comparison between the proposed approach and the baseline model, illustrating the average performance across the entire population. The PCA-based approach, without altering the modal frequencies, demonstrates near-perfect results. This is expected since the reduction of stiffness directly affects the modal frequencies, and the PCA effectively captures this dependency. When a Gaussian alteration with a 0.2 Hz standard deviation is introduced (half of the

TABLE II. SUMMARY OF PERFORMANCE FOR BOTH APPROACHES

	Proposed Approach (DSAS)				Baseline		
					All modes		mode 8 removed
Anomaly level	No noise	30 dB	18dB	10dB	0 std	0.2 std	0.2 std
0%	0.5	0.51	0.50	0.5	0.5	0.5	0.5
1%	0.59	0.53	0.53	0.51	0.99	0.55	0.5
3%	0.87	0.67	0.57	0.52	0.99	0.76	0.54
5%	0.99	0.79	0.64	0.56	0.99	0.93	0.59
7%	0.99	0.87	0.72	0.6	0.99	0.98	0.66
9%	0.99	0.92	0.78	0.67	0.99	0.99	0.74
11%	1.00	0.94	0.82	0.72	1.00	0.99	0.80
13%	1.00	0.96	0.89	0.78	1.00	0.99	0.89

PSD resolution), the baseline model's performance declines and becomes comparable to DSAD method. The performance of DSAD method declines with an 18 dB noise level, mainly due to the final mode being inundated by noise. To ensure a fair comparison, we remove this mode's eigenfrequency from the baseline model, leading to comparable performance once again. Figure 7 illustrates a control chart for one of the systems in the population, constructed using the 1$^{\text{st}}$ scenario (no noise). The vertical lines on the chart represent different anomaly levels. The lower control limit (LCL) is established using the training healthy data, calculated as the mean minus 3 standard deviations, and is depicted as a horizontal line. Notably, a 1% anomaly level is detectable, corresponding to an AUC of 0.65 (low AUC) for this particular system. This demonstrate that in the SHM context a low AUC e.g. 0.65 is acceptable. This outcome provides evidence supporting the effectiveness of our approach in detecting anomalies, even with presence of noise.

CONCLUSION

In conclusion, this study presents a novel anomaly detection method for PB-SHM, eliminating manual feature engineering and environmental variable measurements. Using deep learning models and PSD as input, our approach offers a comprehensive view of a structure's state. Tested on 20 simulated 8-DOF systems, the method shows potential for PB-SHM in environments with variability. Comparing favorably to resonance frequency methods, our approach could excel in complex structures with multiple modes. Future research could involve Bayesian neural networks, different types of anomalies and real structure data.

Data Availability

The processed data (PSD) for the four noise scenarios can be found on Zenodo [20]. The code used to generate the time domain data, process it, and train the models is available in [21].

REFERENCES

1. Alokita, S., V. Rahul, K. Jayakrishna, V. Kar, M. Rajesh, S. Thirumalini, and M. Manikandan. 2019. "Recent advances and trends in structural health monitoring," *Structural health monitoring of biocomposites, fibre-reinforced composites and hybrid composites*:53–73.
2. Amezquita-Sanchez, J. P. and H. Adeli. 2016. "Signal processing techniques for vibration-based health monitoring of smart structures," *Archives of Computational Methods in Engineering*, 23:1–15.
3. Deraemaeker, A., E. Reynders, G. De Roeck, and J. Kullaa. 2008. "Vibration-based structural health monitoring using output-only measurements under changing environment," *Mechanical systems and signal processing*, 22(1):34–56.
4. Tibaduiza Burgos, D. A., R. C. Gomez Vargas, C. Pedraza, D. Agis, and F. Pozo. 2020. "Damage identification in structural health monitoring: A brief review from its implementation to the use of data-driven applications," *Sensors*, 20(3):733.
5. Tcherniak, D. and L. L. Mølgaard. 2015. "Vibration-based SHM system: application to wind turbine blades," in *Journal of Physics: Conference Series*, IOP Publishing, vol. 628.
6. Carden, E. P. and P. Fanning. 2004. "Vibration based condition monitoring: a review," *Structural health monitoring*, 3(4):355–377.
7. Magalhães, F. and Á. Cunha. 2011. "Explaining operational modal analysis with data from an arch bridge," *Mechanical systems and signal processing*, 25(5):1431–1450.
8. Weil, M., W. Weijtjens, and C. Devriendt. 2022. "Autoencoder and Mahalanobis distance for novelty detection in structural health monitoring data of an offshore wind turbine." in *Journal of Physics: Conference Series*, IOP Publishing, vol. 2265.
9. Zhao, R., R. Yan, Z. Chen, K. Mao, P. Wang, and R. X. Gao. 2019. "Deep learning and its applications to machine health monitoring," *Mechanical Systems and Signal Processing*, 115:213–237.
10. Bel-Hadj, Y. and W. Weijtjens. 2022. "Anomaly detection in vibration signals for structural health monitoring of an offshore wind turbine," in *European Workshop on Structural Health Monitoring: EWSHM 2022-Volume 3*, Springer, pp. 348–358.
11. Bull, L., P. Gardner, J. Gosliga, T. Rogers, N. Dervilis, E. Cross, E. Papatheou, A. Maguire, C. Campos, and K. Worden. 2021. "Foundations of population-based SHM, Part I: Homogeneous populations and forms," *Mechanical systems and signal processing*, 148:107141.
12. Yang, J., K. Zhou, Y. Li, and Z. Liu. 2021. "Generalized out-of-distribution detection: A survey," *arXiv preprint arXiv:2110.11334*.
13. Welch, P. 1967. "The use of fast Fourier transform for the estimation of power spectra: a method based on time averaging over short, modified periodograms," *IEEE Transactions on audio and electroacoustics*, 15(2):70–73.
14. Virtanen, P., R. Gommers, T. E. Oliphant, M. Haberland, T. Reddy, D. Cournapeau, E. Burovski, P. Peterson, W. Weckesser, J. Bright, et al. 2020. "SciPy 1.0: fundamental algorithms for scientific computing in Python," *Nature methods*, 17(3):261–272.
15. Pearce, T., A. Brintrup, and J. Zhu. 2021. "Understanding softmax confidence and uncertainty," *arXiv preprint arXiv:2106.04972*.
16. Song, J., Y. Song, and S. Ermon. 2019. "Unsupervised out-of-distribution detection with batch normalization," *arXiv preprint arXiv:1910.09115*.
17. Goodfellow, I., Y. Bengio, and A. Courville. 2016. *Deep learning*, MIT press.
18. McInnes, L., J. Healy, and J. Melville. 2018. "Umap: Uniform manifold approximation and projection for dimension reduction," *arXiv preprint arXiv:1802.03426*.
19. Cattell, R. B. 1966. "The scree test for the number of factors," *Multivariate behavioral research*, 1(2):245–276.

20. 2023. *Population-Based SHM Under Environmental Variability Using a Classifier for Unsupervised Damage Detection*, Zenodo, doi:10.5281/zenodo.7907087.
21. Bel-Hadj, Y. and W. Weijtjens. 2023, "YacineBelHadj/PBSHM_mdof: IWSHM contribution," doi:10.5281/zenodo.7912820.